The role of stress induced martensite in ductile metastable Beta Ti-alloys showing combined TRIP/TWIP effects

F. Sun, J. Y. Zhang, C. Brozek, M. Marteleur, M. Véron, E. Rauch, T. Gloriant, P. Vermaut, C. Curfs, P. J. Jacques, et al.

Available online at www.sciencedirect.com

ScienceDirect

materialstoday: PROCEEDINGS

Materials Today: Proceedings 2S (2015) S505 – S510

International Conference on Martensitic Transformations, ICOMAT-2014

The role of stress induced martensite in ductile metastable Beta Ti-alloys showing combined TRIP/TWIP effects

F. Sun[a,*], J.Y. Zhang[a], C. Brozek[a], M. Marteleur[b], M. Veron[c,d], E. Rauch[c,d], T. Gloriant[e], P. Vermaut[a], C. Curfs[f], P. J. Jacques[b], F. Prima[a,*]

[a]*Institut de Recherche de Chimie Paris, CNRS UMR 8247– Chimie ParisTech, 11 rue Pierre et Marie Curie, 75005 Paris, France*
[b]*Université Catholique de Louvain, IMAP, Place Sainte Barbe 2, B-1348 Louvain-la-Neuve, Belgium*
[c]*Université Grenoble Alpes, SIMAP, F-38000 Grenoble, France*
[d]*CNRS, SIMAP, F-38000 Grenoble, France*
[e]*Institut des Sciences Chimiques de Rennes, UMR CNRS 6226, INSA de Rennes, 20 avenue des Buttes de Coësmes, F-35043 Rennes, France*
[f]*European Synchrotron Radiation Facility (ESRF), Grenoble, France*

Abstract

A new family of metastable beta type titanium alloys has recently been designed for ductility improvement with large strain-hardening effect. Superior plastic properties were obtained due to collective effects of both phase transformation induced plasticity and twinning induced plasticity. A series of stress induced phase transformations, including stress/strain-induced beta to omega transformation and stress-induced martensitic beta to α'' transformations, play particular roles at each deformation stage. The SIM transformations were found to be closely related to the strain-hardening behavior of the material. In this work, the relationship between SIM transformations and strain-hardening effect were studied by microstructural investigations.

Selection and Peer-review under responsibility of the chairs of the International Conference on Martensitic Transformations 2014.

Keywords: Titanium alloys; Martensitic phase transformation; Mechanical twinning; Microstructure; Deformation mechanism

* Corresponding author. Tel.: +33-143-548-702; fax: + 33-144-276-710.
E-mail address: sunfan82@gmail.com, frederic.prima@chimie-paristech.fr

Selection and Peer-review under responsibility of the chairs of the International Conference on Martensitic Transformations 2014.
doi:10.1016/j.matpr.2015.07.336

1. Introduction

Titanium and its alloys have been attracting increasing attentions due to their combination of properties such as high strength [1, 2], low density, biocompatibility and good corrosion resistance [1, 3]. Among them, β-metastable titanium alloys keep exhibiting attractive compromise regarding resistance/ductility combination through the occurrence of several possible deformation mechanisms such as dislocation slip, mechanical twinning and stress induced phase precipitation, as a function of the β phase stability [4-9]. In the past ten years, a large part of scientific work has been dedicated to elastic properties, developing new β-type alloys with ultra-low Young's modulus and/or superelastic properties for biomedical applications [10-17]. Recently, an electronic design approach for the development of a new family of titanium alloys exhibiting a combination of high ductility and improved strain hardening rate has been proposed and exemplified in the model alloys: binary Ti-12Mo (wt.%) grade [18, 19] and the ternary Ti-9Mo-6W (wt.%) grade. The chemical formulation of such alloys was designed following the Morinaga model [20-22] based on the cluster DV-Xα method by mapping electronic parameters Bo (bond order) and Md (*d*-orbital energy).

In the case of the high strain-hardening rate in the model alloys, the design approach aims at activating simultaneously various deformation modes. It is well known that, in titanium alloys, the main deformation mechanism evolves from dislocation glide to mechanical twinning then to martensitic transformation when the β phase chemical stability decreases. Domains corresponding to the transition between these two last deformation modes have then been targeted on the Bo/Md map. In this paper, the experimental validation of this design procedure is performed, revealing true stress - true strain values at necking, of about 1100MPa and 0.38, respectively, with a large strain-hardening rate close to the theoretical limit**.** These values of strength and elongation were hardly reached before in BCC alloys. Both mechanical twinning and stress/strain induced phase transformations were observed in deformed samples, in good agreement with the theoretical predictions. Furthermore, the role of stress-induced martensitic (SIM) α'' phase transformation is characterized in a synergetic relationship with mechanical twinning in stabilizing the plastic flow.

2. Experimental

The model alloys ingots were processed by the arc-melting technique. Plates of 10mm in thickness were cut, followed by solution treatment (ST) at 950 ºC for 30 minutes and water quenching. The specimens were then cold rolled down to 0.5mm thick sheets. These sheets were finally recrystallized at 950 ºC for 30 minutes and water quenched to restore a fully β state.

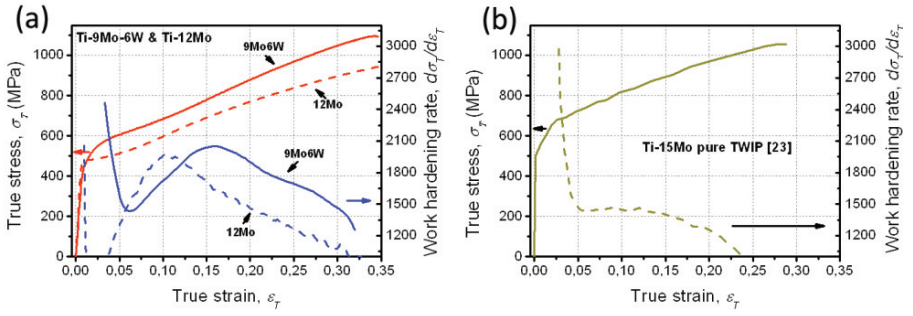

Fig. 1. (a) The true stress-true strain curves of the designed alloys, Ti-12Mo and Ti-9Mo-6W, exhibiting excellent ductility and very good strain-hardening effect. (b) The true stress-true strain curve and strain-hardening rate curve of a Ti-15Mo alloy, exhibiting pure TWIP effect without TRIP effect [23].

In-situ synchrotron X-ray diffraction data were collected at the high-resolution beam line ID31 of the European Synchrotron radiation Source (ESRF), Grenoble (France), from a tensile sample with gauge width of 4 mm and 0.5 mm in thickness.

Specimens deformed to various strains were also prepared for electron backscattered diffraction (EBSD) and transmission electron microscopy (TEM). EBSD scans were performed using a field emission gun scanning electron microscope operating at 15 kV, with step sizes ranging from 0.1 to 0.05 μm. A JEOL 2000FX transmission electron microscope operating at 200 kV was used for conventional microstructural investigation. A JEOL 3010 TEM operated at 300 kV was used to perform automatic crystal orientation measurements (ACOM-TEM) with an ASTAR^{TM} system [23]. The orientation/phase identification was performed by diffraction pattern matching algorithm to reconstruct the deformation microstructure.

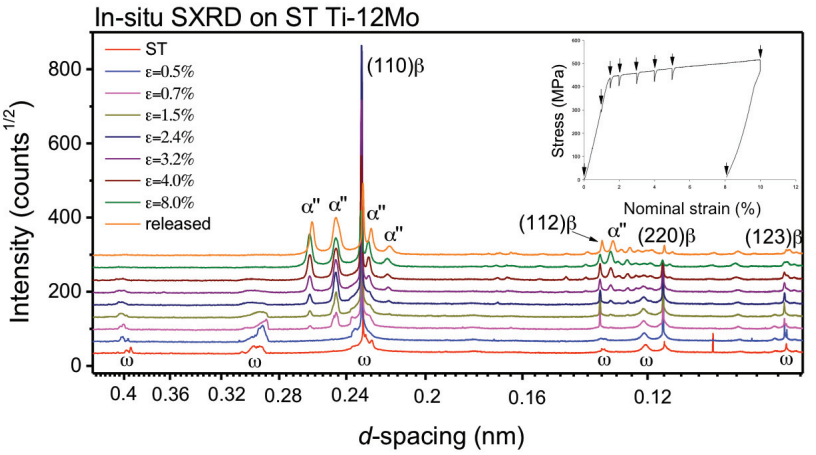

Fig. 2. *In-situ* synchrotron x-ray diffraction (SXRD) patterns corresponding to increasing deformation levels. The stress/strain curve is shown in the inset [19].

3. Results and discussions

3.1. Validation of design strategy on TRIP/TWIP effect

The mechanical behaviors of the designed alloys were examined by uniaxial tensile test. Excellent ductility and very high strain-hardening rate were observed (shown in Fig. 1) as expected. In order to verify the activated phase transformations upon deformation (TRIP effect), *in-situ* synchrotron XRD was performed on a ST Ti-12Mo specimen. As shown in Fig. 2, strong α'' signals were detected from ε=0.007, the onset of plastic regime, until ε=0.08. The intensity of the α'' peaks is increasing along with the applied strain. The main phase transformation induced by stress is β-> α'' martensite, which proves the activation of TRIP effect. On the other hand, the mechanical twinning was identified by the TEM microstructural investigation on deformed specimen. Fig. 3 shows a deformation twinning band along [011] β zone axis with an edge-on winning interface. The corresponding SAED pattern on the interface identified a twinning configuration of twinning plane of (2-33)β and twinning direction of [31-1]β, which is the typical twinning system {332}<113> in metastable β Ti-alloys. It can be noticed that the TWIP and TRIP effects are activated simultaneously in the designed alloys. The activation sequence and early stage deformation mechanisms have been investigated in detail in one of our previous works [19]. The results have shown that the deformation microstructure is composed by the combination of a transgranular {332}<113> twinning network (primary twinning) and thin SIM α'' plates precipitated near the β twins (primary α'') and inside the twinned β zones (secondary α''). A combined mechanism, dynamic Hall-Petch effect (twinning network) and composite effect (TWIP+TRIP), has been concluded as a reasonable explanation of the unusual strain-hardening rate and the subsequent superior ductility in BCC alloys. Thus, the design strategy is validated by the combined TWIP/TRIP mechanisms.

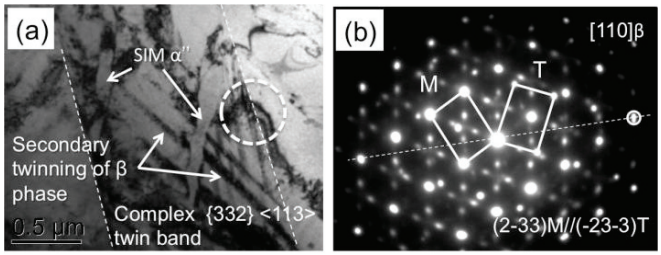

Fig. 3. TEM characterization of the deformation twinning in the deformed alloys (ε=0.05). (a) Bright-field image of a mechanical twin; (b) the corresponding selected area electron diffraction (SAED) pattern on the twinning interface identifies a (2-33)[31-1] twinning relationship.

3.2. The role of SIM in the combined TRIP/TWIP effect

It can be noticed clearly that the ductility and strain-hardening rate of the designed alloys, showing combined TWIP and TRIP effects, are very different from the performances of a Ti-15Mo alloy [24], showing only TWIP effect (Figs. 1a and 1b). The activation of SIM in the plastic range seems effectively improving the uniform plasticity and enhancing the strain-hardening effect. In order to clarify the role of TRIP effect in the total contribution of the combined effects, dedicated microstructural investigations were performed. A confinement effect of the α'' precipitates was observed, leading to reasonable hypotheses on the role of α'' in strain-hardening effect. The strain-hardening rate may probably benefit from the three confined phenomena: (i) 2nd α'' occupation; (ii) α'' cluster; and (iii) composite band of α'' + twinning. The EBSD mapping (Fig. 4) demonstrated three microstructural features, 2nd SIM α'' in β twins, the "dark clusters" and "composite band", numbered by 1, 2 and 3, respectively. It can be noticed that the β grain was divided into separated regions by the networking of deformation-induced bands. Interestingly, no β twinning bands were identified in the map but several α'' plates. By measuring the crystallographic relationship between the α'' plates and the nearby β matrix, no conventional relationship can be determined. In fact, the α'' martensite was precipitated in {332}<113> β twins, fully or partially occupying the twinned β zones. It is unusual that such precipitation shows a typical confinement effect, preferring the nucleation and growth of martensite in very limited volume (β twins with high misorientation interfaces). The mechanism of such preference is still unclear besides several assumptions on orientation preference, size effect or defect density. Nevertheless, one consequence can be assured is that the nature of the twin band, e.g. on responding the dislocation reactions on the twin interfaces and on local strain misfit state, would be seriously influenced, resulting in the first hypothesis: the confined α'' occupation at β twins would probably contribute to the strain-hardening rate and ductility by enhancing the macroscopic dynamic H-P effect and the composite effect.

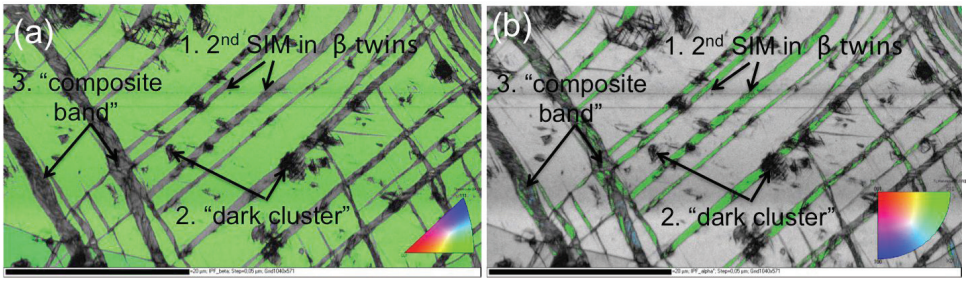

Fig. 4. EBSD orientation contrast imaging of the deformed alloy (ε=0.05). (a) orientation map of β phase; (b) orientation map of SIM α'' precipitates. Three microstructural features are shown in the figure: 2nd SIM α'' in β twins, the "dark clusters" and "composite band", numbered by 1, 2 and 3, respectively.

The question following the first microstructural feature would be obvious that where locates the primary SIM α'' phase? The labeled "2. dark clusters" (Fig. 4) would answer the question by showing confined clusters of needle-like SIM α'' plates. The detailed microstructural works were realized by using ACOM-TEM technology and

HRTEM imaging. Fig. 5a shows the orientation mapping of the SIM α'' variants. An assumption of the contribution of such α'' clusters to the mechanical performance is suggested based on the emission of dislocations from the enormous interfaces. Evidences were found by HRTEM investigations on these interfaces (Fig. 5b). Therefore, the second hypothesis of the role of α'' can be fairly addressed that the confined α'' clusters serves as sources of dislocations, which helps to stabilize the deformation flow in a synergetic way with twinning network.

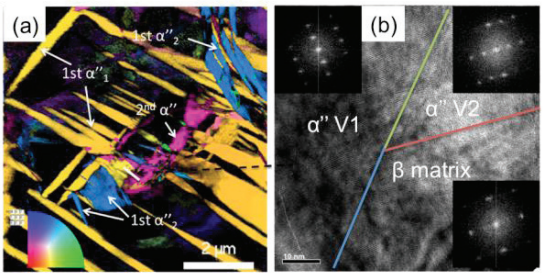

Fig. 5. TEM characterizations on the feature "dark clusters", (a) ACOM-TEM orientation mapping of SIM α'' variants; (b) HRTEM imaging of a joint position among two α'' variants and β matrix.

The synergy effect between TRIP and TWIP can be further exemplified by the third microstructural feature, the "3. composite band" (indicated in Fig. 4). Fig. 6 demonstrates a "composite band" by TEM bright-field imaging. Detailed analysis by using ACOM-TEM technology (the NBD scanning) illustrates the delicate composition of the band's complexity. The band is actually constructed by the components of 1st {332}<113> twins and 1st α'' precipitates in a synergistic configuration (illustrated by blocks in Fig. 5b). Still, these tiny twin components are also highly preferred by the occupation of 2nd α'' phase, resulting in a continuous deformation bands showing a composition of different α'' variants (typical EBSD mapping features in all specimens at micrometric scale). No evidences have been found, by us or from literatures, so far on the influences of such "composite band" to the general mechanical behaviors of the material. However, if we consider this traversing band as a divider of the grain, then not less significant (at least equivalent) contributions to the dynamic H-P effect could be suggested when comparing to the mechanical twins.

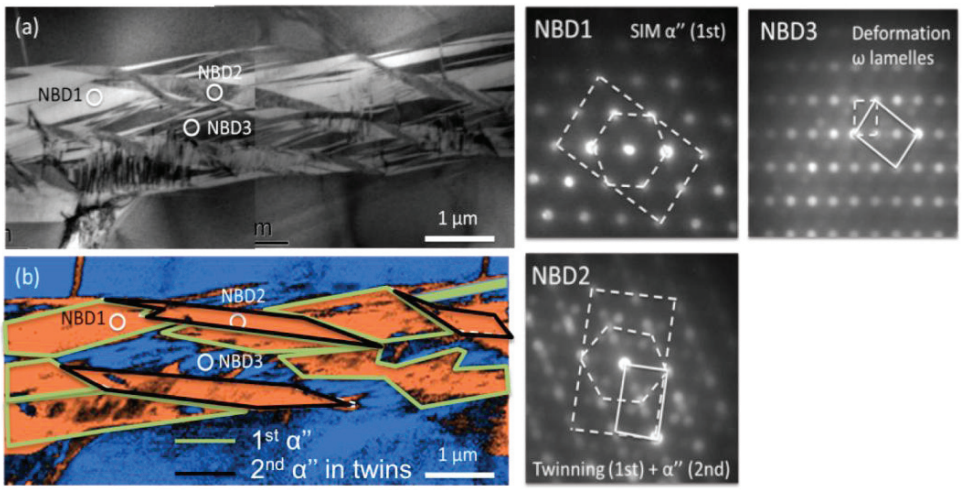

Fig. 6. TEM characterizations on the feature "composition band", (a) TEM bright-field image of the "composite band"; (b) ACOM-TEM phase mapping of SIM α'' (orange) and β phase (blue). The key NBD patterns of each zone of interest are also given. A schematic drawing of the different phase blocks are added onto the (b) ACOM-TEM mapping [25].

4. Conclusions

The design strategy of the TWIP/TRIP Ti-alloys is validated by model alloys and other designed alloys. The excellent strain hardening and ductility are due to the synergetic effect between SIM and mechanical twinning. The role of SIM in the combined TWIP/TRIP behavior was investigated by microscopic analysis. The main contributions of SIM are improving strain hardening rate and stabilizing the plastic flow. The corresponding mechanisms can be concluded in manner of a general confinement effects of the SIM α'' precipitation: (i) secondary α'' occupation in the twinned beta zone; (2) clusters of nanometric needle-like α'' plates; (3) a composite band constructed by components of primary {332}<113> twins and α'' variants.

Acknowledgements

Fan SUN would like to thank the committee of ICOMAT 2014 for the great opportunity of "Invited lecture" on behave of Laboratory of Structural Metallurgy from Chimie-Paristech, France.

References

[1] J.C. Williams, E.A. Starke Jr., Acta Mater. 51 (2003) 5775-5799.
[2] D. Banerjee, J.C. Williams, Acta Mater. 61 (2013) 844-879.
[3] T.C. Niemeyer, C.R. Grandini, L.M.C. Pinto, A.C.D. Angelo, S.G. Schneider, J. Alloy. Compd. 476 (2009) 172-175.
[4] T. Grosdidier, M.J. Philippe, Mater. Sci. Eng. A 291 (2000) 218-223.
[5] A. Gysler, G. Lutjering, V. Gerold, Acta Metall. 22 (1974) 901-909.
[6] H.Y. Kim, Y. Ikehara, J.I. Kim, H. Hosoda, S. Miyazaki, Acta Mater. 54 (2006) 2419-2429.
[7] H. Xing, J. Sun, Appl. Phys. Lett. 93 (2008) 031908-031908-031903.
[8] E. Bertrand, P. Castany, I. Péron, T. Gloriant, Scr. Mater. 64 (2011) 1110-1113.
[9] S. Hanada, O. Izumi, Metall. Mater. Trans. A 17 (1986) 1409-1420.
[10] F. Sun, S. Nowak, T. Gloriant, P. Laheurte, A. Eberhardt, F. Prima, Scr. Mater. 63 (2010) 1053-1056.
[11] P. Laheurte, F. Prima, A. Eberhardt, T. Gloriant, M. Wary, E. Patoor, J. Mech. Behav. Biomed. 3 (2010) 565-573.
[12] Y.L. Hao, S.J. Li, S.Y. Sun, C.Y. Zheng, R. Yang, Acta Biomater. 3 (2007) 277-286.
[13] S. Miyazaki, H. Kim, H. Hosoda, Mater. Sci. Eng. A 438-440 (2006) 18-24.
[14] F. Sun, Y.L. Hao, S. Nowak, T. Gloriant, P. Laheurte, F. Prima, J. Mech. Behav. Biomed. 4 (2011) 1864-1872.
[15] Y. Al-Zain, H.Y. Kim, T. Koyano, H. Hosoda, T.H. Nam, S. Miyazaki, Acta Mater. 59 (2011) 1464-1473.
[16] Y.L. Hao, S.J. Li, F. Prima, R. Yang, Scr. Mater. 67 (2012) 487-490.
[17] J.Y. Zhang, F. Sun, Y.L. Hao, N. Gozdecki, E. Lebrun, P. Vermaut, R. Portier, T. Gloriant, P. Laheurte, F. Prima, Mater. Sci. Eng. A 563 (2013) 78-85.
[18] M. Marteleur, F. Sun, T. Gloriant, P. Vermaut, P.J. Jacques, F. Prima, Scripta Mater. 66 (2012) 749-752.
[19] F. Sun, J.Y. Zhang, M. Marteleur, T. Gloriant, P. Vermaut, D. Laillé, P. Castany, C. Curfs, P.J. Jacques, F. Prima, Acta Mater. 61 (2013) 6406-6417.
[20] M. Abdel-Hady, K. Hinoshita, M. Morinaga, Scripta Mater. 55 (2006) 477-480.
[21] M. Morinaga, N. Yukawa, T. Maya, K. Sone, H. Adachi, 6th World Conf. on Titanium III, 6-9 June 1988, Cannes, 1988, pp. 1601-1606.
[22] D. Kuroda, M. Niinomi, M. Morinaga, Y. Kato, T. Yashiro, Mater. Sci. Eng. A 243 (1998) 244-249.
[23] E. Rauch, M. Véron, J. Portillo, D. Bultreys, Y. Maniette, S. Nicolopoulos, Micro. Anal. UK (2008) S5.
[24] X.H. Min, X. Chen, S. Emura, K. Tsuchiya, Scr. Mater. 69 (2013) 393–396.
[25] F. Sun, J.Y. Zhang, M. Marteleur, C. Brozek, E.F. Rauch, M. Véron, P. Vermaut, P.J. Jacques, F. Prima, Scr. Mater. 94 (2015) 17–20.